Accepted refereed manuscript of: Wang X, Jin M, Cheng X, Hu X, Zhao M, Yuan Y, Sun P, Jiao L, Tocher DR, Betancor MB & Zhou Q (2022) Lipidomic profiling reveals molecular modification of lipids in hepatopancreas of juvenile mud crab (Scylla paramamosain) fed with different dietary DHA/EPA ratios. *Food Chemistry*, 372, Art. No.: 131289.
https://doi.org/10.1016/j.foodchem.2021.131289

Lipidomic profiling reveals molecular modification of lipids in hepatopancreas of juvenile mud crab (*Scylla paramamosain*) fed with different dietary DHA/EPA ratios

Xuexi Wang[a], Min Jin[a]*, Xin Cheng[a], Xiaoying Hu[a], Mingming Zhao[a], Ye Yuan[a], Peng Sun[a], Lefei Jiao[a], Douglas R. Tocher[b], Mónica B. Betancor[c], Qicun Zhou[a]*

[a] Laboratory of Fish and Shellfish Nutrition, School of Marine Sciences, Ningbo University, Ningbo 315211, China

[b] Guangdong Provincial Key Laboratory of Marine Biotechnology, Institute of Marine Sciences, Shantou University, Shantou 515063, China

[c] Institute of Aquaculture, Faculty of Natural Sciences, University of Stirling, Stirling FK9 4LA, United Kingdom

* Corresponding author:

E-mail address:

jinmin@nbu.edu.cn (M. Jin);

zhouqicun@nbu.edu.cn (Q. -C. Zhou)

Abstract

Untargeted lipidomic analysis was conducted to explore how different dietary docosahexaenoic acid (DHA) / eicosapentaenoic acid (EPA) ratio and, specifically, how an optimal ratio (2.3) compared to a suboptimum ratio (0.6) impacted lipid molecular species and the positional distribution of fatty acids in hepatopancreas of mud crab. The results indicated that major category of lipid affected by dietary DHA/EPA ratio was glycerophospholipids (GPs). The optimum dietary DHA/EPA ratio increased the contents of DHA bound to the *sn-2* and *sn-3* positions of phosphatidylcholine (PC) and triacylglycerol, EPA bound to the *sn-2* position of phosphatidylcholine and 18:2n-6 bound to the *sn-2* position of phosphatidylethanolamine (PE). Increased dietary DHA/EPA ratio also led to competition between arachidonic acid (ARA) and 18:2n-6 bound to esterified sites. Appropriate dietary DHA/EPA ratio can not only improve the growth performance and nutritional quality of mud crab, but also provide higher quality products for human consumers.

Key words: *Scylla paramamosain,* DHA/EPA, Untargeted lipidomics, Lipid molecules, Fatty acid composition, Positional distribution.

1. Introduction

Most animals cannot synthesize the polyunsaturated fatty acids (PUFA), linoleic acid (LA, 18:2n-6) and α-linolenic acid (LNA, 18:3n-3) from the precursor oleic acid (18:1n-9), and they have to be obtained in the diet. In addition, the metabolic conversion of LNA and LA to long-chain polyunsaturated fatty acids (LC-PUFA) such as arachidonic acid (ARA, 20:4n-6), eicosapentaenoic acid (EPA, 20:5n-3) and docosahexaenoic acid (DHA, 22:6n-3) is poor in marine animals, and hence dietary uptake is significantly more effective. However, marine animal species including fishes, shrimps, prawns, crabs and shellfish are rich in EPA and DHA. Usually, microalgae are the primary source of n-3 LC-PUFA for marine fish and shellfish. Thus, in mud crab *Scylla paramamosain*, PUFA represent 51.0% - 62.5% of total fatty acids with most being the n-3 LC-PUFA such as EPA and DHA (Li, Zhao, Li, Wang, Mu, Song, et al., 2019). The mud crab is widely distributed in coastal Malaysia, Vietnam, Japan and China, it has become the major marine crustacean farmed in China in recent years (Wang, Jin, Cheng, Luo, Jiao, Betancor, et al., 2021). According to the China Fishery Statistical Yearbook (2020), production of farmed mud crabs was over 160 thousand tons in 2019, mainly *S. paramamosain*. In Asia, the hepatopancreas and ovaries of the marine or freshwater crabs are prized for their delicious and unique taste.

The hepatopancreas in crustaceans is central to lipid metabolism and plays critical roles in growth and reproduction, especially during ovarian development. During the processes of molting and reproduction abundant lipids are accumulated and deposited in the hepatopancreas of crustaceans (Wang, Wu, Liu, Zheng, & Cheng, 2014). Lipids in crustaceans hepatopancreas not only supply energy, but also provide essential fatty acids to maintain the integrity of cell membranes and other metabolic roles, and cholesterol for the synthesis of molting hormones (Harrison, 1990).

Generally, the two predominant lipid classes in tissues are triacylglycerols (TGs) that are the major neutral lipid and perceived as an energy reserve, whereas glycerophospholipids (GPs) are important polar lipids that are the main components of biological membranes and implicated in a variety of cellular functions (Lykidis, 2007). The GPs are critical for lipid absorption, transportation and deposition and are a rich source of LC-PUFA, therefore, are also precursors of eicosanoids, diacylglycerol inositol phosphates and other highly biologically active mediators, which play important metabolic and physiological functions (Tocher, Bendiksen, Campbell & Bell, 2008). Phosphatidylcholine (PC), phosphatidylethanolamine (PE) and phosphatidylinositol (PI) are quantitatively the most important GPs in animal tissues which play key roles in regulating membrane structure, fluidity, signal transduction and lipid metabolism (Vance & Tasseva, 2013). While TG molecules consist of a glycerol backbone esterified with three fatty acids at *sn-1*, *sn-2* and *sn-3* positions, typical GP molecules such as PC, PE and PI share a common structure consisting of two fatty acids esterified at the *sn-1* and *sn-2* positions of the glycerol moiety, with phosphate and a base (e.g. choline, ethanolamine or inositol) esterified to *sn-3*. The location of fatty acids on the glycerol backbone is important for lipid and fatty acid utilization and hydrolysis (Liu, Jiao, Gao, Ning, Limbu, Qiao, et al., 2019; Xu, Wei, Xie, Lv, Dong, & Chen, 2018). Importantly, the fatty acid composition of lipids in tissues including hepatopancreas or liver usually reflects dietary fatty acid profiles (Unnikrishnan & Paulraj, 2010), which means that the fatty acid compositions of lipids in mud crab hepatopancreas can be modified by diet. However, there is little information about the impact that dietary DHA/EPA ratio could have in modifying composition and structure of lipid molecules in the hepatopancreas of mud crab.

High-resolution mass spectrometry (MS), such as quadrupole time-of-flight MS and

quadrupole Exactive Orbitrap (Q-Exactive Orbitrap), with extremely high resolution, sensitivity, and mass precision has recently been applied to the non-target lipid analysis of various food matrices such as milk, meat and fish (Li, Zhao, Zhu, Pang, Liu, Frew, et al., 2017; Mi, Shang, Li, Zhang, Liu, & Huang, 2019; Wang, Zhang, Song, Cong, Li, Xu, et al., 2019). The advanced analytical technique of MS combined with highly selective ultra-performance liquid chromatography (UPLC) enables hundreds of lipids to be separated and identified in an unbiased way (Li, Liang, Xue, Wang, & Wu, 2019; Lim, Long, Mo, Dong, Cui, Kim, et al., 2017) and so lipidomics has developed rapidly in recent years. However, lipidomic studies on crustacean lipids are limited up to now, therefore, the objective of present study was conducted to use an MS-based lipidomic approach to investigate how dietary DHA/EPA ratio affects the abundance and structures of lipid molecules in hepatopancreas for mud crab. The overall aim is to provide novel insights into lipid nutrition and metabolism of crustaceans, and improve the culture and nutritional quality of farmed mud crab.

2. Materials and methods

2.1. Ethics statement

This study was conducted in strict compliance with the Standard Operation Procedures of the Guide for Use of Experimental Animals of Ningbo University. Specific protocols and procedures in the experiment were endorsed by the Institutional Animal Care and Use Committee of Ningbo University.

2.2. Diets

Four purified diets containing approximately 45% crude protein and 7% crude lipid were formulated with DHA:EPA ratios of approximately 1:2, 1:1, 2:1 and 3:1 and named D1, D2, D3 and D4, respectively (Wang, Jin, Cheng, Hu, Zhao, Yuan, et al., 2021). The experimental diets were

manufactured as described in detail previously (Wang, Jin, Cheng, Luo, Jiao, Betancor, et al., 2021), after which the air-dried diets were kept at -20 °C prior to use. The detailed formulations and proximate compositions of the diets are presented in Supplemental Table 1 and the fatty acid profiles are presented in Supplemental Table 2. The average total n-3 LC-PUFA content of the experimental diets was 19.2 mg g^{-1} diet dry weight and ranged between 18.5 and 20.0 mg g^{-1} with final DHA : EPA ratios of 0.6, 1.2, 2.3 and 3.2, respectively.

2.3. Feeding trial and sampling

A total of 120 healthy juvenile mud crabs (20.92 ± 0.56 g $crab^{-1}$) were obtained from Jia-Shun Aquatic-Cooperatives (Taizhou, China) and the feeding trail carried out in single crab cells (0.33 m × 0.23 m × 0.15 m, length × width × height) at the Ningbo Marine and Fishery Science and Technology Innovation Base (Ningbo, China). Crabs were randomly divided into triplicate groups with 10 crabs per replicate and 3 replicates per dietary treatment to give 30 crabs per treatment. The conditions in cells were stable and as follows: temperature 26 - 30 °C, salinity 26 - 28 g L^{-1}, pH 7.7 - 8.0, dissolved oxygen 6.5 - 7.0 mg L^{-1}, and ammonia nitrogen was lower than 0.05 mg L^{-1}. Further details of the management of the 8-week feeding trial were presented previously (Wang, Jin, Cheng, Hu, Zhao, Yuan, et al., 2021).

At the end of the 8-week feeding period, 18 crabs were selected randomly from each dietary treatment (6 crabs per replicate). The hepatopancreas was dissected from each crab and pooled from 3 crabs to provide a total of 6 samples per dietary treatment. Approximately 500 mg of each pooled sample was taken and stored at -80 °C prior to untargeted lipidomic analysis (n = 6 per dietary treatment). The remaining of the pooled hepatopancreas (6 per dietary treatment) was immediately frozen and stored at -20 °C prior to the analysis of fatty acid composition (n = 3 per dietary

126 treatment).

127 *2.4. Preparation of fatty acid methyl esters (FAME) and analysis of fatty acid composition by gas*
128 *chromatography (GC)*

129 In brief, total lipid was extracted from approximately 100 g of diets and freeze-dried
130 hepatopancreas samples using chloroform/methanol (2:1, v:v) according to Bligh & Dyer, (1959)
131 and as described in previous study (Rey, Alves, Melo, Domingues, Queiroga, Rosa, et al., 2015).
132 Approximately 10 mg of total lipid were placed in a glass test tube along with 1 mL of 23:0 internal
133 standard solution (1 mg mL^{-1}, in HPLC grade hexane > 95%), and dried by Termovap TV10 sample
134 concentrator (Ecom, Czech Republic). Three mL methanolic sulfuric acid solution (1 mL H_2SO_4 :
135 100 mL methanol : 0.05 g butylated hydroxytoluene [BHT; as antioxidant]) were added to the glass
136 tubes that were then incubated in a water bath at 80 ℃ for 3 h to produce FAME. One mL hexane
137 and distilled water were added and the mixture vortexed for 1 min and cooled to room temperature.
138 The upper layer was filtered through a lipid phase filter (SCAA-104, ANPEL, China) and the solvent
139 evaporated under a stream of nitrogen and FAME dissolved in 0.5 mL hexane. The FAME samples
140 were analyzed on a GC (GC-MS 7890B-5977A, Agilent Technologies, USA) with the GC-MS
141 operating conditions as described previously (Yuan, Xu, Jin, Wang, Hu, Zhao, et al., 2021). Fatty
142 acids were identified by their retention time in comparison to a FAME standard solution (FAME 37
143 MIX, Supelco), and fatty acid concentrations calculated according to the peak area ratio of
144 FAME/23:0 standard.

145 *2.5. Lipid preparation and extraction*

146 Briefly, 25 mg of hepatopancreas sample was defrosted at 4 ℃ in a mircofuge tube,
147 resuspended in 800 μL dichloromethane/methanol (3:1, v:v) and 10 μL internal standard stock

148 (SPLASH 330707, SPLASHTM Lipidomix Mass Spec Standard, Avanti Polar Lipids, USA), and
149 then incubated at -20 ℃ for 1 h.. Following centrifugation at 25 000 rpm for 15 min at 4 ℃, 600
150 μL of supernatant was concentrated by vacuum concentrator (Maxi Vacbeta, GENE COMPANY).
151 The concentrates were resuspended in 200 μL of isopropanol/acetonitrile/H_2O (2:1:1, v:v:v),
152 vortexed for 1 min and incubated at room temperature for 10 min, were stored into -80 ℃ until
153 further analysis.

154 *2.6. UPLC-MS method for lipidomics*

155 Lipidomic analysis was carried out using a Waters 2D UPLC (Waters, Milford, MA, USA)
156 coupled to a Q-Exactive Orbitrap MS (Thermo Fisher Scientific, USA) with electrospray ionization
157 (ESI). The lipids of hepatopancreas samples were separated on a UPLC charged surface hybrid C18
158 column (2.1 × 100 mm, 1.7 μm; Waters) with a mobile phase consisting of a mixture of 10 mM
159 ammonium formate in acetonitrile/water (60:40, v:v; A) with a gradient of 10 mM ammonium
160 formate in isopropanol/acetonitrile (90:10, v:v; B) in ESI^- mode. For ESI^+ mode, the same A and B
161 solutions containing 0.1% formic acid were used. In both cases the mobile phase was delivered at a
162 flow rate of 0.35 mL min^{-1} with the column initially eluted with 60% A and 40% B. The proportion
163 of B increased to 43% over 2 min, then rapidly to 50% (0.1 min), then linearly to 54% over 4.9 min,
164 before rapidly increasing to 70% (0.1 min), before a final linear gradient to 99% over 5.9 min in the
165 last section of the gradient. The percentage of B solution percentage decreased back to 40% (0.1
166 min) and the column equilibrated for 2 min before the next sample injection.

167 Primary data were obtained using the full scan mass-to-charge ratio range of the Q-Exactive
168 Orbitrap MS of 200 to 2000 with 70,000 of the primary resolution, 3e6 automatic gain control (AGC)
169 and 100 ms maximum injection time. Secondary level data were acquired by fragmenting the top

three highest intensity precursor ions with 15, 30 and 45 eV of stepped normal collision energies, 17,500 of the secondary resolution, 1e5 AGC and 50 ms maximum injection time. The parameters of ESI mode of MS were set as follows: 40 sheath gas flow rate, 10 auxiliary gas flow rate, 320 ℃ capillary temperature, 350 ℃ auxiliary gas heater temperature and 3.80 (3.20) spray voltage for ESI^+ (ESI^-) mode. In order to determine the stability of data, a QC sample was run and analyzed every ten samples.

2.7. High quality non-targeted metabolic profile acquisition and metabolite identification

The raw MS datasets were imputed into commercially available software, LipidSearch v.4.1 (Thermo Fisher Scientific, USA), to identify peaks on a single sample, and then perform peak alignment on all samples. As for identifying lipids, the mass tolerances for molecular precursors, product and fragment ions were all set at 5 ppm, the thresholds of m-score and c-score were set to 5.0 and 2.0. The adducts form were $[M+H]^+$, $[M+NH_4]^+$ and $[M+Na]^+$ for ESI^+ mode, and $[M-H]^-$, $[M-2H]^-$ and $[M-HCOO]^-$ for ESI^- mode. Peak alignment was then performed on all the identified lipids, with deviation of retention time set at 0.1 min. The grade of identification levels were A, B, C and D where grade A represented the lipid category and all fatty acid chains completely determined, for grade B both class specific ions and fatty acid fragment ions could be detected, for grade C either class-specific ions or fatty acid fragment ions could be detected, and for grade D the lipid structure could not be recognized, such as dehydrated ions. The discovery of outlier and assessment of batch effects was carried out by principal component analysis (PCA) of the dataset being pre-processed (Supplemental Figure 2). The standardized peak data was further analyzed using metaX, the process of which included 1) removing lipids that were observed in less than 50% of QC or 80% of biological samples, 2) filling missing values using k-Nearest Neighbor algorithm,

3) normalizing data to gain relative peak area using the method of probabilistic quotient normalization, 4) deleting lipid molecules with a coefficient of variation of relative peak area > 30%. The high-resolution LC-MS/MS features were then identified using Progenesis QI 2.0 by searching in the public databases including Human Metabolome Database (HMDB), LIPID MAPS Structure Database (LMSD).

2.8. Statistical analyses

The data for growth performance and fatty acid compositions were presented as means ± SEM (n = 3). The lipidomic data were presented as means ± SEM (n = 6). Data were first analyzed using one-way analysis of variance (ANOVA) using SPSS 23.0 (SPSS, IBM, USA). Student's t-test was applied for comparison of the lipidomic data between the two treatments with dietary DHA/EPA ratios of 0.6 and 2.3. PCA and partial least squares discriminant analysis (PLS-DA) was processed by SIMCA-P + 14.0 software package (Umetrics, Umea, Sweden). Cluster heatmaps were performed using MultiExperiment viewer (MEV, version 4.9.0).

3. Results and Discussion

3.1. Growth performance, fatty acid composition in hepatopancreas and expression of genes related to LC-PUFA biosynthesis

The growth performance of mud crabs fed with diets containing different DHA/EPA ratios is presented in Supplementary Table 3. Molting frequency (MF) was not influenced significantly by dietary DHA/EPA ratios although it was numerically higher in crabs fed with diet containing 2.3 of dietary DHA/EPA ratio. Crabs fed with diets containing 0.6 and 2.3 of DHA/EPA ratios respectively showed the lowest and highest weight again (WG) and specific growth rate (SGR) among all

214 treatments. Based on second-order polynomial regression analysis of WG against dietary DHA/EPA
215 ratio, 2.2 was determined to be the optimum ratio for mud crab fed with 7% lipid (Supplementary
216 Fig. 1). This was higher than that reported previously in juvenile *P. trituberculatus*, where 0.7 - 0.8
217 was estimated to be the optimum dietary DHA/EPA ratio although this was with a diet containing
218 11% lipid (Hu, Wang, Han, Li, Jiang, & Wang, 2017). However, 2.0 was also reported to be the
219 optimum dietary DHA/EPA ratio for swimming crab fed with 11% lipid during ovarian development
220 (Feng, 2011). In addition, 2.0 - 3.0 was determined to be the optimum range for this ratio in Chinese
221 mitten crab (*Eriocheir sinensis*) fed with 7.5% lipid (Zhao, 2013). These studies indicated that a
222 precise dietary DHA/EPA ratio is essential to fulfil requirements for growth and development but
223 that the ratio varied with culture species, diet formulation and lipid content, and developmental stage
224 (NRC, 2011).

225 The fatty acid content and relative expression of genes involved to LC-PUFA biosynthesis in
226 hepatopancreas are presented in Figure 1 and Supplementary Table 4. In crustaceans, while the
227 hepatopancreas is the center of lipid metabolism, fatty acid composition generally reflects that of
228 diet. In the present study, significantly higher contents of total FA, total SFA, total MUFA and total
229 n-6 PUFA were observed in crabs fed with diet D2 and D3 than in crabs fed with diet D1 and D4.
230 The lowest content of total n-3 PUFA was shown in crabs fed with diet D1, and the content of DHA
231 and the DHA/EPA ratio in hepatopancreas both increased significantly as dietary DHA/EPA ratio
232 increased. This may simply be a consequence of the greater retention of DHA compared to other
233 fatty acids including EPA (Tocher et al., 2010), but may also reflect the greater biological value of
234 DHA (Carvalho, Peres, Saleh, Fontanillas, Rosenlund, Oliva-Teles, et al., 2018). Thus, compared to
235 crabs fed with the lowest dietary DHA/EPA ratio (D1), higher dietary DHA/EPA ratios up to 2.3

significantly promoted the growth of mud crab and improved the nutritional value of hepatopancreas by increasing DHA and overall n-3 LC-PUFA contents.

Insert Figure 1 here

3.2. Composition of lipid classes in hepatopancreas

Based on weight gain, a dietary ratio of DHA/EPA of approximately 2 was estimated to be optimum for juvenile mud crab fed with 7% lipid diet (Supplemental Figure 1) (Wang, Jin, Cheng, Hu, Zhao, Yuan, et al., 2021). Therefore, in the present study, samples of hepatopancreas from crabs fed with diet D1 (lowest growth) and D3 (optimal growth) were used to evaluate the effects of dietary DHA/EPA ratio on the distribution and composition of lipid using untargeted lipidomics. Supplementary Figures 3 and 4 show representative Q-Exactive plus mass spectra in ESI^+ and ESI^- modes of QC and experimental samples, respectively, which confirmed the high stability of the system and reliability of the data. The number and content (%) of lipid categories and classes in hepatopancreas are shown in Figure 2. After removal duplicate molecules, a total of 390 unique lipid molecular species belonging to a total of 22 lipid classes in 4 major categories (GPs, fatty acyls, glycerolipids and sphingolipids) were identified. Specifically, 15 lipid classes represented by 336 lipid species (i.e. 86% of all identified species) were GPs including 144 PCs, 76 PEs, 28 PSs, 27 PIs, 18 LPCs and others. Thus, the major lipid metabolites found in hepatopancreas of mud crab fed with diet D1 and D3 containing 0.6 and 2.3 of dietary DHA/EPA ratios were GPs, which was similar to the results reported for hepatopancreas of *P. trituberculatus* and muscle of *Sagmariasus verreauxi* fed with different lipid sources (Shu-Chien, Han, Carter, Fitzgibbon, Simon, Kuah, et al., 2017; Yuan, et al., 2021). The relative contents of lipid classes in hepatopancreas were generally not affected by the diet, however the absolute contents of fatty acids were significantly affected by

dietary DHA/EPA ratio, therefore it was necessary to detect the different lipid metabolites (DLMs).

Insert Figure 2 here

3.3. Identification of DLMs

Principal component analysis was used to observe clustering trends simultaneously to identify and exclude outliers in the data (Figure 3). In addition, PLS-DA was used for building a discriminant model with validity and potential over-fitting of the model checked by performing 200 permutation tests and visualization using a validation plot (Supplementary Figure 6). A Volcano plot was used to show the difference in lipid metabolites (Figure 3). The components of lipid species in hepatopancreas of crabs fed with diet D1 and D3 were clustered as two groups and separated from each other with no overlap. The lipid metabolites with fold change (FC) ≥ 1.20 or ≤ 0.83 ($log_2FC \geq 0.26$ or ≤ -0.27), $P < 0.05$ and Variable Importance in Projection (VIP) ≥ 1 were defined as DLMs. Compared to crabs fed with diet containing a dietary DHA/EPA ratio 0.6, a total of 77 DLMs with 47 up-regulated and 30 down-regulated were identified in hepatopancreas of crabs fed with diet D3 containing an optimum DHA/EPA ratio of 2.3 (Figure 3C). Figure 3D showed that PC (54%) species contributed greatly to the difference between D1 and D3, followed by PE (14%) and PI (13%) species. Previously it was reported that the predominant DLMs in hepatopancreas of *P. trituberculatus* and fillets of Nile tilapia (*Oreochromis niloticus*) fed with different lipid sources were TG, PC and PE (Liu, et al., 2019; Yuan, et al., 2021). Differences in the predominant DLMs between the studies may be due to crab species, diet formulation including dietary lipid content and composition, and further analysis of DLMs in different species and trials should be conducted to further evaluate the importance and role of dietary changes to lipid metabolites.

Insert Figure 3 here

3.4. Analysis of the predominant DLMs in hepatopancreas

In order to further investigate the effects of dietary DHA/EPA ratio on the distribution of lipid metabolites, PLS-DA and clustering heatmap were used to discriminate the composition of all the predominant DLMs and analyze the variation in these lipid species identified in hepatopancreas of crabs fed with diet D1 and D3. In the present study, the PLS-DA plot (Figures 4A, B and C and Supplementary Figure 6) showed the distinctions and trends in PC, PE and PI molecules. All the samples were within the 95% Hotelling T^2 ellipse, and samples from the two diets were separated from each other, indicating the significant difference between metabolites in hepatopancreas of crabs fed with diet D1 and D3 containing suboptimal and optimal DHA/EPA ratio, respectively. Cluster heatmap analysis showed more comprehensive and intuitive distribution pattern and relationship of lipid metabolites between the samples of the two dietary groups, which was helpful to evaluate the rationality of different lipid metabolites. The clustering heatmap (Figures 4D, E and F) showed the variation in the PC, PE and PI molecular species directly, which confirmed the result of PLS-DA. The heatmap also showed that the 6 replicates of the same group and lipid metabolites containing the same fatty acid were well clustered. For example, PC molecules containing DHA were positively correlated with the dietary ratio of DHA/EPA. The results indicated that the molecular compositions of PC, PE and PI of crab hepatopancreas were significantly affected by dietary DHA/EPA ratio. However, TG also plays a key role in cellular biology, organ function and lipid metabolism and is the main form for deposition and storage of fatty acids (Goldberg, 2012; Stubhaug, Tocher, Bell, Dick, & Torstensen, 2005). Considering that the location of fatty acids on the glycerol backbone of lipid metabolites is important for lipid and fatty acid utilization and hydrolysis, the compositions of TG and the predominant glycerophospholipid classes, PC, PE and

PI, were analyzed further.

Insert Figure 4 here

3.5. The distribution of key fatty acids in TG, PC, PE and PI in hepatopancreas

Figure 5 shows the positional distribution of 16:0, 18:1n-9, 18:2n-6, ARA, EPA and DHA in different TG, PC, PE and PI. Although, TG (18:0/20:4/22:6) and TG (18:1/18:1/22:5) were the only two neutral glycerolipid species in DLMs found in the present study, the contents of 18:1n-9 and ARA combined were significantly higher in TG than in PC, PE and PI (Figure 5), indicating TG was the main class for deposition of these fatty acids in mud crab hepatopancreas. The deposition of 18:1n-9 at the *sn-1* position was lower than that at the *sn-2* position of PE molecules in crabs fed with diet D3, while the opposite trends were observed in the deposition of 16:0 and 18:1n-9 in PC and PI molecules in crabs fed with both diet D1 and D3. It was reported that an excess intake of lipid containing 16:0 at the *sn-2* position may increase the risk of atherogenesis, whereas fatty acids at the *sn-1/3* positions are preferred for pancreatic lipase and are readily lipolyzed (Mattson & Volfenhein, 1962). Monounsaturated fatty acid, especially 18:1n-9 is generally regarded as "healthy" fat in human nutrition (Grundy, 1989). It has been shown that 18:1n-9, especially bound to TG, is better for suppling energy via β-oxidation than n-3 LC-PUFA (Du, Araujo, Stubhaug, & Frøyland, 2010). Figure 6 shows that the content of 16:0 bound at the *sn-1* position of PC was higher, and 18:1n-9 bound at *sn-2* position of PC and *sn-1* and *sn-2* positions of TG were lower in crabs fed with diet D3 containing optimal DHA/EPA ratio than crabs fed with diet D1 containing a suboptimal ratio. This suggested that 18:1n-9 could be a good supply of energy and that SFA and MUFA tend to bind the *sn-1* position of lipid molecules and, most importantly in terms of the present study, that mud crabs fed with the diet containing optimum DHA/EPA ratio (2.3) are recommended for

consumption compared to crabs fed with a suboptimum ratio (0.6).

The positional distribution of other fatty acids in DLMs were similar, with the contents of 18:2n-6, ARA, EPA and DHA higher at the *sn-2* position than at *sn-1* position of lipid molecules in hepatopancreas of crabs fed with both diet D1 and D3, other than ARA in PC in crabs fed with diet D1 where no difference was observed in the deposition between *sn-1* and *sn-2* (Figure 5). It has been long accepted that fatty acids bound at the *sn-2* position are more stable than those at *sn-1/3* and so the results indicate *sn-2* is the predominant binding site for LC-PUFA in hepatopancreas of *S. paramamosain* irrespective of diet contributing to its high nutritional value, and similar results were reported previously in a lipidomic study on *O. niloticus* fed with different dietary oils (Liu, et al., 2019). However, significantly different (DLM) TG had DHA preferentially bound at *sn-3* rather than *sn-1* and *sn-2* positions, suggesting sufficient DHA may be bound at the *sn-2* position of TG in crabs fed with diet D1 and D3, and higher intake of DHA in crabs fed with diet D3 was bound at the *sn-3* position. A previous study reported that seal oil had high anti-inflammatory effects due to EPA and DHA being predominantly bound at the *sn1/3* positions (Christensen et al., 1995). The present study may also indicate that mud crabs fed with diet containing optimal dietary DHA/EPA ratio may have increased anti-inflammatory capacity for humans consuming the crabs. In contrast, 18:2n-6 at the *sn-1/3* positions could be more easily hydrolyzed and might lead to inflammation (Naughton, Mathai, Hryciw, & McAinch, 2016). In the present study, the content of 18:2n-6 at the *sn-1* and *sn-2* position of PC was lower and at *sn-2* position of PE was higher in hepatopancreas of crabs fed with diet D3 containing optimal DHA/EPA ratio than crabs fed with diet D1 containing suboptimal ratio. Combined with the higher 18:2n-6 content in crabs fed with diet D3, these results showed that the *sn-2* position of PE was the predominant binding site for 18:2n-6. Similarly, 18:2n-

346 6 was specifically deposited at the *sn-2* position of PC and PE in *O. niloticus* (Liu, et al., 2019).
347 Moreover, the risk of inflammation for consumption of mud crab hepatopancreas may be low, and
348 could be further decreased by feeding an optimum dietary DHA/EPA ratio (Figure 6).

349 Importantly, the contents of ARA at *sn-1* and *sn-2* positions of PC were significantly higher in
350 crabs fed with diet D3 than crabs fed with diet D1, whereas the content of ARA at the *sn-2* position
351 of PE showed the opposite (Figure 6). Interestingly, the opposite trends were also observed between
352 contents of ARA and 18:2n-6 at the same binding site of PC and PE, which may indicate competition
353 between ARA and 18:2n-6 for esterification sites and/or the biosynthesis of ARA from 18:2n-6 in *S.*
354 *paramamosain,* both worthwhile topics for further study. The contents of EPA at *sn-1* in PC and *sn-*
355 *2* in PE were significantly lower, and at *sn-2* in PC significantly higher, in crabs fed with diet D3
356 than crabs fed with diet D1. It was reported previously that LC-PUFA at the *sn-2* positions of PC
357 and PE increase the fluidity of cell membranes (van der Veen, Kennelly, Wan, Vance, Vance, &
358 Jacobs, 2017) and the present study has demonstrated that an optimal dietary DHA/EPA ratio
359 promoted this function in mud crab. The contents of DHA in PC, PI and TG molecules were higher
360 in hepatopancreas of crabs fed with diet D3 than in crabs fed with diet D1 (Figure 6), moreover, the
361 content of DHA bound at the *sn-2* position of PC was higher than that bound at the *sn-3* position of
362 TG (Figure 5). When taking the changes of ARA, EPA and DHA contents in lipid molecules and
363 hepatopancreas into consideration (Figure 1 and Supplementary Table 4), we speculate that ARA,
364 EPA and DHA are preferentially stored at the *sn-2* position of PC molecules in hepatopancreas of
365 mud crab. In contrast, a previous study demonstrated that DHA was preferentially deposited in PE
366 molecules in the muscle of largemouth bass (*Micropterus salmoides*) (Zhang, 2019). Given that the
367 species are different and relevant research in crustaceans are few, further studies still require to be

368 conducted.

369 Insert Figure 5 here

370 Insert Figure 6 here

371 **4. Conclusions**

372 In the present study, the results of lipidomic analysis revealed that the major lipids in
373 hepatopancreas affected by dietary DHA/EPA ratios were glycerophospholipids (GPs). Irrespective
374 of diet, ARA, EPA and DHA were preferentially located at the *sn-2* position PC molecules while
375 SFA and MUFA tended to be bound at the *sn-1* position of lipid molecules in hepatopancreas of
376 mud crab. The *sn-2* position of PE was the predominant binding site for 18:2n-6. The optimum
377 dietary DHA/EPA ratios increased the contents of ARA, EPA and DHA bound to the *sn-2* position
378 of PC molecules, the content of 18:2n-6 bound to the *sn-2* position of PE molecules, and the content
379 of DHA bound to the sn-3 position of TG, potentially improve the anti-inflammatory properties of
380 mud crab hepatopancreas when consumed. Increased dietary DHA/EPA ratio may lead to
381 competition between ARA and 18:2n-6 bound to esterified sites. To the best of our knowledge, this
382 is the first study investigated the impact of dietary DHA/EPA ratio in modifying the species
383 composition of lipid molecules in hepatopancreas. Overall, optimal dietary DHA/EPA ratio could
384 not only improve the culture of *S. paramamosain* potentially providing economic benefits, but also
385 increase the nutritive value of farmed crab providing health benefits for human consumers.

386 **Acknowledgments**

387 This research was supported by National Key R & D Program of China (2018YFD0900400),
388 China Agriculture Research System-48 (CARS-48), Nature Science Foundation of Zhejiang
389 Province (LY17C190002), Key Research Program of Zhejiang Province of China (2018C02037),

Zhejiang Aquaculture Nutrition & Feed Technology Service Team (ZJANFTST2017-2). This research was also sponsored by the K. C. Wong Magna Fund in Ningbo University. The authors graciously thank Ningbo Institute of Materials Technology and Engineering, Chinese Academy of Sciences (NIMTE, CAS) for use of the Agilent Technologies GC-MS 7890B-5977A, USA.

CRediT authorship contribution statement

Xuexi Wang: Conceptualization, Data curation, Formal analysis, Investigation, Methodology, Project administration, Validation, Visualization, Writing-original draft. **Min Jin:** Formal analysis, Resources, Supervision, Writing-review & editing. **Xin Cheng:** Investigation, Methodology. **Xiaoying Hu:** Investigation, Methodology. **Mingming Zhao:** Investigation, Methodology. **Ye Yuan:** Software, Visualization. **Peng Sun:** Software, Visualization. **Lefei Jiao:** Software, Visualization. **Douglas R. Tocher:** Formal analysis, Writing-review & editing. **Mónica B. Betancor:** Writing-review & editing. **Qicun Zhou:** Conceptualization, Formal analysis, Funding acquisition, Resources, Supervision, Writing-review.

& editing.

Declaration of competing interest

The authors declare that they have no competing financial interests or personal relationships that could have appeared to influence the work reported in this paper.

Supplementary data

Supplementary Table 1. Formulations and proximate compositions of the experimental diets.

412 **Supplementary Table 2.** Fatty acid contents (mg g^{-1}, dry matter) of the experimental diets

413 **Supplementary Table 3.** Growth performance of mud crabs fed with the experimental diets.

414 **Supplementary Table 4.** Fatty acid contents (mg g^{-1}, dry matter) of hepatopancreas of mud crabs
415 fed with the experimental diets.

416 **Supplementary Figure 1.** Optimal dietary DHA/EPA requirement of mud crab fed with 7% lipid.

417 **Supplementary Figure 2.** Principal component analysis (PCA) plots for QC samples.

418 **Supplementary Figure 3.** The overlap plot of base peak chromatograms (BPC) acquired in positive
419 (A) and negative (B) ionization mode of all the quality control samples.

420 **Supplementary Figure 4.** The base peak chromatograms (BPC) acquired in positive (A) and
421 negative (B) ionization mode of hepatopancreas of mud crab fed with diet D1 and D3.

422 **Supplementary Figure 5.** Cross-validation plot of the PLS-DA model of all lipid species.

423 **Supplementary Figure 6.** Cross-validation plot of PLS-DA model of PC, PE and PI.

424

425 **References**

426 Carvalho, M., Peres, H., Saleh, R., Fontanillas, R., Rosenlund, G., Oliva-Teles, A., & Izquierdo, M.
427 (2018). Dietary requirement for n-3 long-chain polyunsaturated fatty acids for fast growth of
428 meagre (*Argyrosomus regius*, Asso 1801) fingerlings. *Aquaculture, 488*, 105-113.

429 Bligh, E. G., & Dyer, W. J. (1959). A rapid method of total lipid extraction and purification.
430 *Canadian journal of biochemistry physiology & Behavior*, 37(8), 911-917.

431 China Fishery Statistical Yearbook, 2019. Compiled by Fishery Bureau of China Agriculture
432 Department. pp. 22.

433 Christensen, M. S., Mortimer, B. C., Høy, C. E., & Redgrave, T. G. (1995). Clearance of

chylomicrons following fish oil and seal oil feeding. *Nutrition Research, 15*(3), 359–368.

Du, Z., Araujo, P., Stubhaug, I., & Frøyland, L. (2010). Unbound DHA causes a high blank value in β-oxidation assay: a concern for in vitro studies. *European journal of lipid science technology and Health Care, 112*(3), 333-342.

Feng, L. (2011). The effect of dietary HUFA on the ovary development, endocrine hormones and tissue biochemical composition of the swimming crab *Portunus trituberculatus*. Dissertation, Shanghai Ocean University, Shanghai (in Chinese with English abstract).

Goldberg, I. J. (2012). Triglyceride, One molecule at the center of health and disease. *Biochimica Et Biophysica Acta, 1821*(5).

Grundy, S. M. (1989). Monounsaturated fatty acids and cholesterol metabolism: implications for dietary recommendations. *The Journal of nutrition, 119*(4), 529-533.

Harrison, K. E. (1990). The role of nutrition in maturation, reproduction and embryonic development of decapod crustaceans: a review. *Journal of Shellfish Research, 9*, 1-28.

Hu, S., Wang, J., Han, T., Li, X., Jiang, Y., & Wang, C. (2017). Effects of dietary DHA/EPA ratios on growth performance, survival and fatty acid composition of juvenile swimming crab (*Portunus trituberculatus*). *Aquaculture Research, 48*(3), 1291-1301.

Jin, M., Wang, M.-Q., Huo, Y.-W., Huang, W.-W., Mai, K.-S., & Zhou, Q.-C. (2015). Dietary lysine requirement of juvenile swimming crab, *Portunus trituberculatus*. *Aquaculture*, 448, 1-7.

Li, Q., Liang, X., Xue, X., Wang, K., & Wu, L. (2019). Lipidomics provides novel insights into understanding the bee pollen lipids transepithelial transport and metabolism in human intestinal cells. *Journal of Agricultural and Food Chemistry, 68*(3), 907-917.

Li, Q., Zhao, Y., Zhu, D., Pang, X., Liu, Y., Frew, R., & Chen, G. (2017). Lipidomics profiling of

goat milk, soymilk and bovine milk by UPLC-Q-Exactive Orbitrap Mass Spectrometry. *Food Chemistry, 224*, 302-309.

Li, Y., Zhao, H., Li, R., Wang, C., Mu, C., Song, W., & Ye, Y. (2019). Comparison of amino acid and fatty acid composition in *Scylla paramamosain* from six different wild populations (in Chinese with English abstract). *Oceanologia et Limnologia Sinica, 50*(2), 465-472.

Lim, D. K., Long, N. P., Mo, C., Dong, Z., Cui, L., Kim, G., & Kwon, S. W. (2017). Combination of mass spectrometry-based targeted lipidomics and supervised machine learning algorithms in detecting adulterated admixtures of white rice. *Food Research International, 100*, 814-821.

Liu, Y., Jiao, J., Gao, S., Ning, L., Limbu, S. M., Qiao, F., Chen, L., Zhang, M., & Du, Z. (2019). Dietary oils modify lipid molecules and nutritional value of fillet in Nile tilapia: A deep lipidomics analysis. *Food Chemistry, 277*, 515-523.

Lykidis, A. (2007). Comparative genomics and evolution of eukaryotic phospholipid biosynthesis. *Progress in Lipid Research, 46*(3-4), 171-199.

Mattson, F., & Volfenhein, R. (1962). Rearrangement of glyceride fatty acids during digestion and absorption. *Journal of Biological Chemistry, 237*, 53-55.

Mi, S., Shang, K., Li, X., Zhang, C., Liu, J., & Huang, D. (2019). Characterization and discrimination of selected China's domestic pork using an LC-MS-based lipidomics approach. *Food Control, 100*, 305-314.

Naughton, S. S., Mathai, M. L., Hryciw, D. H., & McAinch, A. J. (2016). Linoleic acid and the pathogenesis of obesity. *Prostaglandins other lipid mediators, 125*, 90-99.

National Research Council (NRC). (2011). *Nutrient Requirements of Fish and Shrimp*. Washington, DC: National Academies Press.

478 Rey, F., Alves, E., Melo, T., Domingues, P., Queiroga, H., Rosa, R., Domingues, M. R. M., & Calado,
479 R. (2015). Unravelling polar lipids dynamics during embryonic development of two sympatric
480 brachyuran crabs (*Carcinus maenas* and *Necora puber*) using lipidomics. *Scientific reports*,
481 5(1), 1-13.
482 Shu-Chien, A. C., Han, W., Carter, C. G., Fitzgibbon, Q. P., Simon, C. J., Kuah, M., Battaglene, S.
483 C., Codabaccus, B. M., & Ventura, T. (2017). Effect of dietary lipid source on expression of
484 lipid metabolism genes and tissue lipid profile in juvenile spiny lobster *Sagmariasus verreauxi*.
485 *Aquaculture, 479*, 342-351.
486 Stubhaug, I., Tocher, D. R., Bell, J. G., Dick, J. R., & Torstensen, B. E. (2005). Fatty acid metabolism
487 in Atlantic salmon (*Salmo salar* L.) hepatocytes and influence of dietary vegetable oil.
488 *Biochimica et Biophysica Acta-Molecular Cell Biology of Lipids, 1734*(3), 277-288.
489 Tocher, D. R. (2010). Fatty acid requirements in ontogeny of marine and freshwater fish.
490 *Aquaculture Research*, *41*, 717-732.
491 Tocher, D. R., Bendiksen, E. Å., Campbell, P. J., & Bell, J. G. (2008). The role of phospholipids in
492 nutrition and metabolism of teleost fish. *Aquaculture, 280*(1-4), 21-34.
493 Unnikrishnan, U., & Paulraj, R. (2010). Dietary protein requirement of giant mud crab *Scylla*
494 *serrata* juveniles fed iso-energetic formulated diets having graded protein levels. *Aquaculture*
495 *Research, 41*(2), 278-294.
496 van der Veen, J. N., Kennelly, J. P., Wan, S., Vance, J. E., Vance, D. E., & Jacobs, R. L. (2017). The
497 critical role of phosphatidylcholine and phosphatidylethanolamine metabolism in health and
498 disease. *Biochimica et Biophysica Acta-Biomembranes, 1859*(9), 1558-1572.
499 Vance, J. E., & Tasseva, G. (2013). Formation and function of phosphatidylserine and

phosphatidylethanolamine in mammalian cells. *Biochimica Et Biophysica Acta Molecular Cell Biology of Lipids, 1831*(3), 543-554.

Wang, W., Wu, X., Liu, Z., Zheng, H., & Cheng, Y. (2014). Insights into hepatopancreatic functions for nutrition metabolism and ovarian development in the crab *Portunus trituberculatus*: gene discovery in the comparative transcriptome of different hepatopancreas stages. *PloS one, 9*(1), e84921.

Wang, X., Jin, M., Cheng, X., Hu, X., Zhao, M., Yuan, Y., Sun, P., Jiao, L., Betancor, M. B., & Tocher, D. R. (2021). Dietary DHA/EPA ratio affects growth, tissue fatty acid profiles and expression of genes involved in lipid metabolism in mud crab *Scylla paramamosain* supplied with appropriate n-3 LC-PUFA at two lipid levels. *Aquaculture, 532*, 736028.

Wang, X., Jin, M., Cheng, X., Luo, J., Jiao, L., Betancor, M. B., Tocher, D. R., & Zhou, Q. (2021). Dietary lipid and n-3 long-chain PUFA levels impact growth performance and lipid metabolism of juvenile mud crab, *Scylla paramamosain*. *British Journal of Nutrition, 125*(8), 876-890.

Wang, X., Zhang, H., Song, Y., Cong, P., Li, Z., Xu, J., & Xue, C. (2019). Comparative lipid profile analysis of four fish species by ultraperformance liquid chromatography coupled with quadrupole time-of-flight mass spectrometry. *Journal of Agricultural Food Chemistry, 67*(33), 9423-9431.

Xu, S. l., Wei, F., Xie, Y., Lv, X., Dong, X. y., & Chen, H. (2018). Research advances based on mass spectrometry for profiling of triacylglycerols in oils and fats and their applications. *Electrophoresis, 39*(13), 1558-1568.

Yuan, Y., Xu, F., Jin, M., Wang, X., Hu, X., Zhao, M., Cheng, X., Luo, J., Jiao, L., & Betancor, M. B. (2021). Untargeted lipidomics reveals metabolic responses to different dietary n-3 PUFA in

juvenile swimming crab (*Portunus trituberculatus*). *Food Chemistry, 354*, 129570.

Zhang, G. (2019). Effects of different lipid sources and protein sources on lipid metabolism and protein metabolism of largemouth bass (*Micropterus salmoides*). Dissertation, Shanghai Ocean University, Shanghai (in Chinese with English abstract).

Zhao, Y. (2013). Effects of dietary dha levels and DHA/EPA ratios on growth and lipid composition of juvenile chinese mitten crab *Eriocheir sinensis*. Dissertation, Shanghai Ocean University, Shanghai (in Chinese with English abstract).

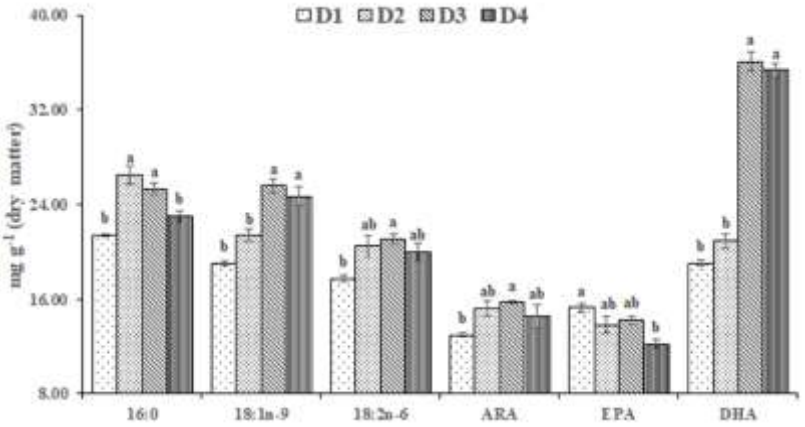

530

531 **Figure 1.** Absolute contents of fatty acids in hepatopancreas of mud crab fed with experiment diets.

532 Values are means ± SEM (n = 3).

533

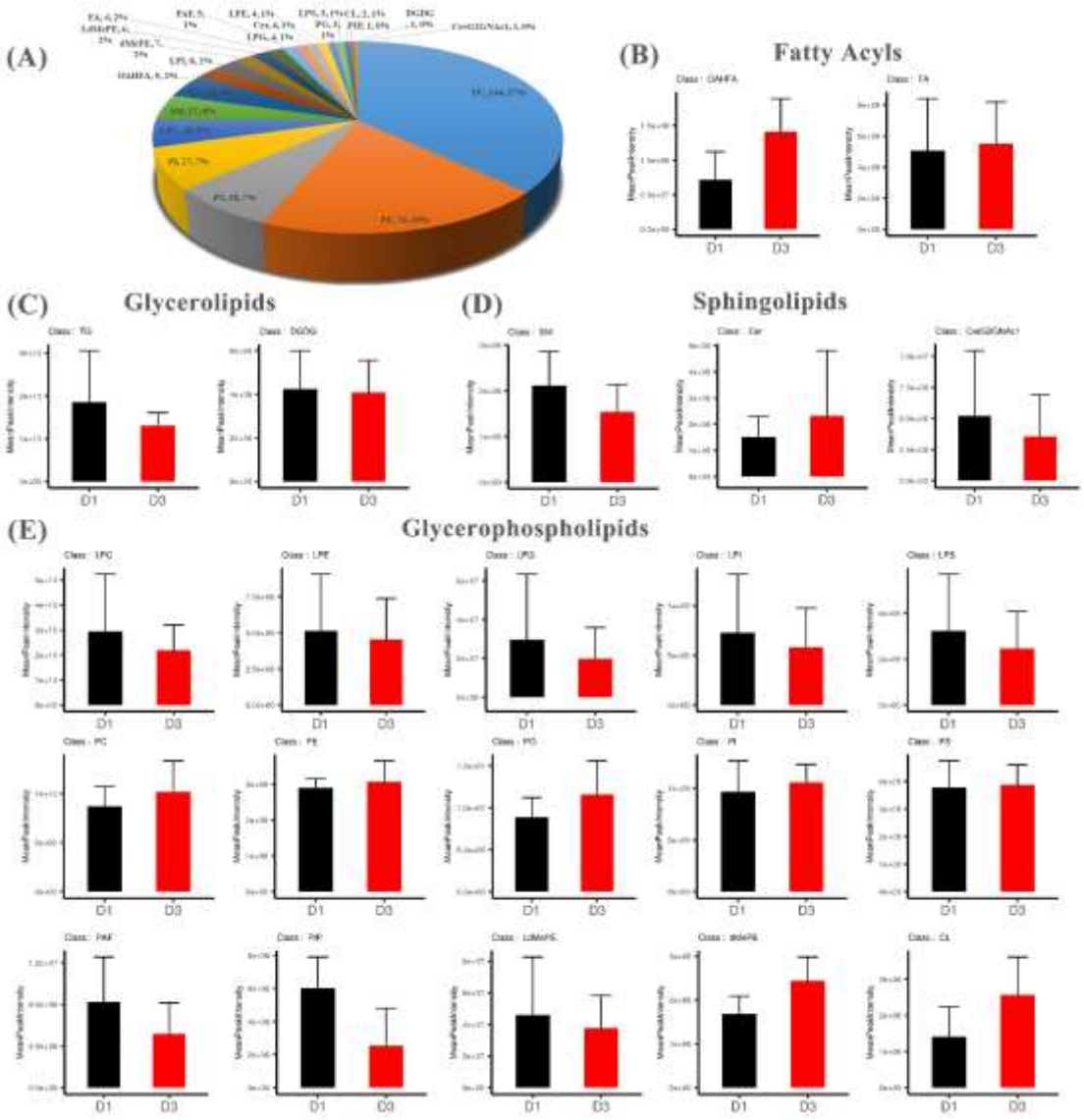

Figure 2. Overall composition and relative contents of lipid classes in hepatopancreas of mud crab fed with diet D1 and D3 containing 0.6 and 2.3 of DHA/EPA. (A) Lipid subclasses, number of lipid molecules identified, and percentage of total. (B-E) Relative contents of lipid classes, (B) fatty acyls, (C) glycerolipids, (D) sphingolipids, (E) glycerophospholipids. Cer, ceramide; CerG2GNAc1, simple Glc series; CL, cardiolipin; DGDG, digalactosyl diacylglycerol; dMePE, Dimethylphosphatidylethanolamine; FA, fatty acid; LdMePE: lysodimethyiphosphatidylethanolamine; LPC, lysophosphatidylcholine; LPE, lysophosphatidylethanolamine; LPG, lysophosphatidylglycerol; LPI, lysophosphatidylinositol; LPS, lysophosphatidylserine; OAHFA, O-acyl- ω -hydroxy fatty acid; PAF, platelet activating factor; PC, phosphatidylcholine; PE, phosphatidylethanolamine; PG, phosphatidylglycerol; PI, phosphatidylinositol; PIP, phosphatidylinositol phosphate; PS, phosphatidylserine; SM, sphingomyelin; TG, triglyceride. Values are means ± SEM (n = 6).

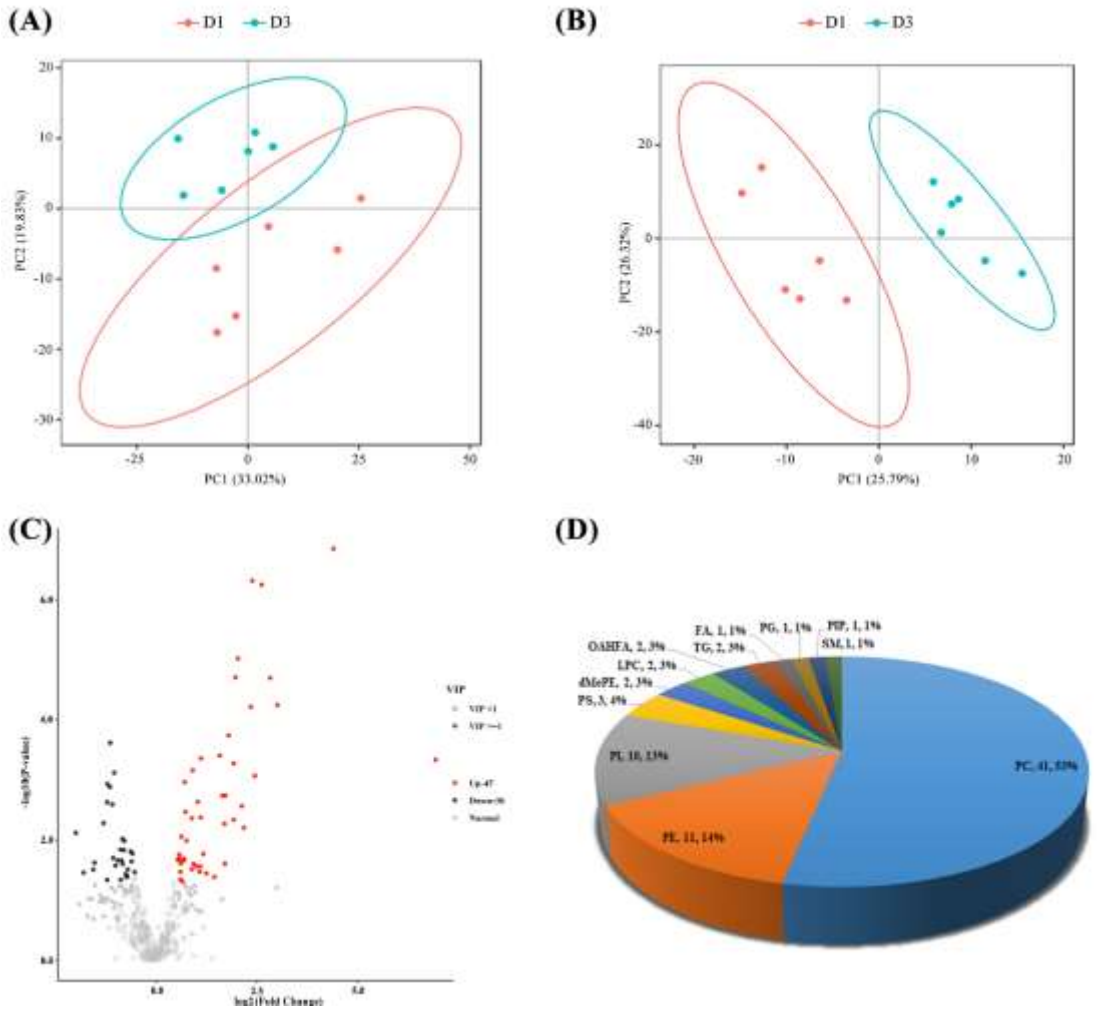

Figure 3. Composition of different lipid metabolites in the hepatopancreas of *S. paramamosain* fed with diet D1 and D3 (DHA/EPA = 0.6 and 2.3, respectively). (A) ● and ● in principal component analysis, PCA (A) and partial least squares method-discriminant analysis, PLS-DA (B) plots represent diets D1 and D3, respectively. In volcano plot (C), • and • represent down-regulated and up-regulated lipid metabolites with $\log_2$(fold change) ≥ 0.26 or ≤ -0.27 and $P < 0.05$, circle and × show lipid metabolites with Variable Importance in Projection (VIP) ≥ 1 and VIP < 1, respectively. (D) the composition of different lipid metabolites (number, percentage).

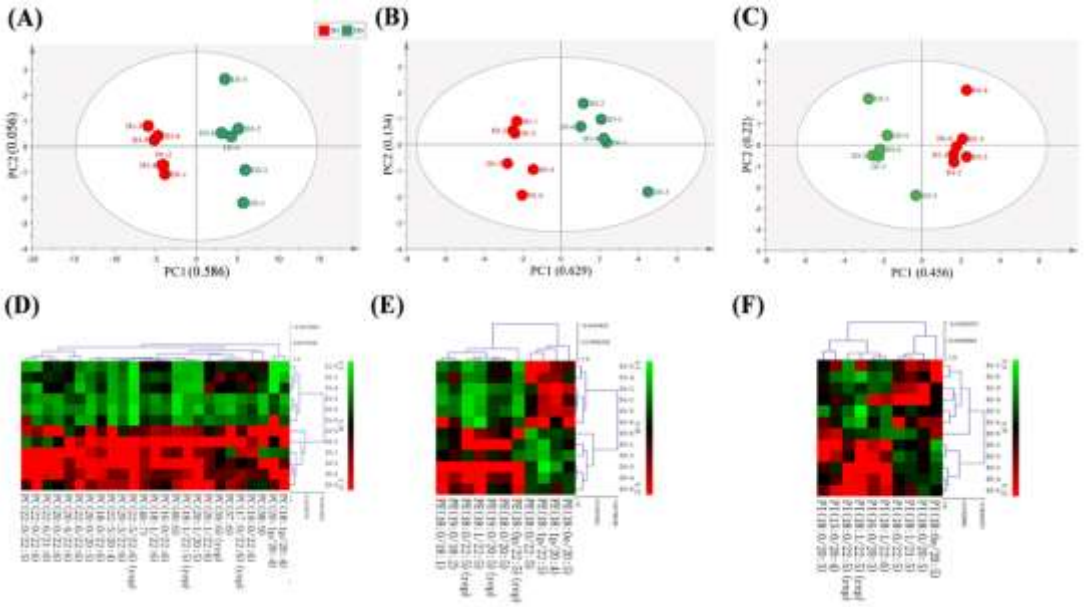

Figure 4. Composition and clustering heatmap of significantly different phosphatidylcholine, PC (A, D), phosphatidylethanolamine, PE (B, E) and phosphatidylinositol, PI (C, F) molecules in the hepatopancreas of *S. paramamosain* fed with diet D1 and D3. ● and ● in PLS-DA plots A, B and C, represent diets D1 and D3, respectively (n = 6). In heatmap plots D, E and F, columns represent different samples; rows represent different lipid molecules, and color change from green to red shows the increase of relative intensity of the lipid molecules.

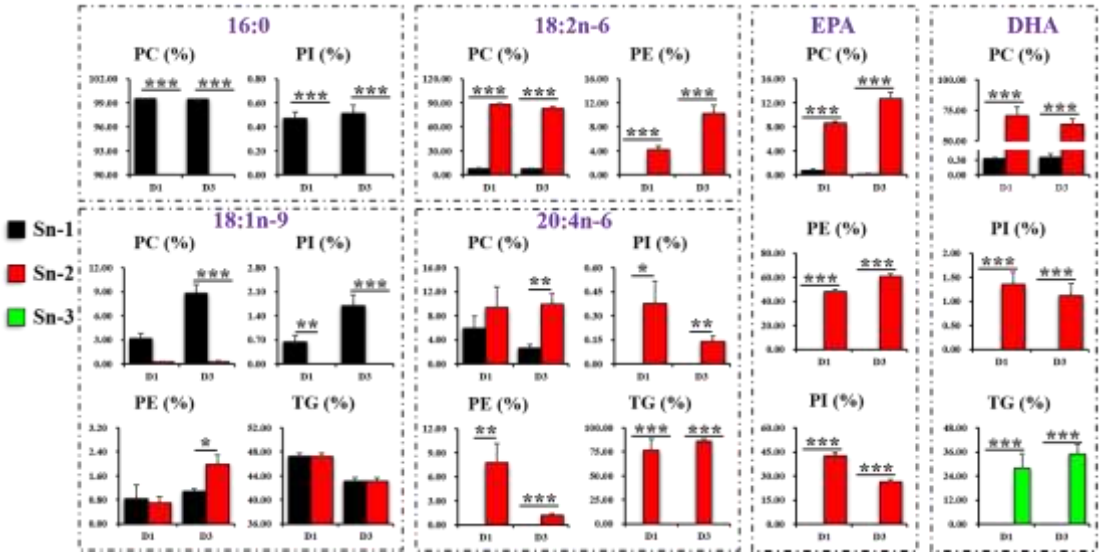

Figure 5. The positional distributions of key fatty acids in phosphatidylcholine (PC), phosphatidylethanolamine (PE), phosphatidylinositol (PI) and triacylglycerol (TG) molecules in hepatopancreas of *S. paramamosain* fed with diet D1 and D3. Values are means ± SEM (n = 6). *, ** and *** represent significant differences with $P < 0.05$, $P < 0.01$ and $P < 0.001$.

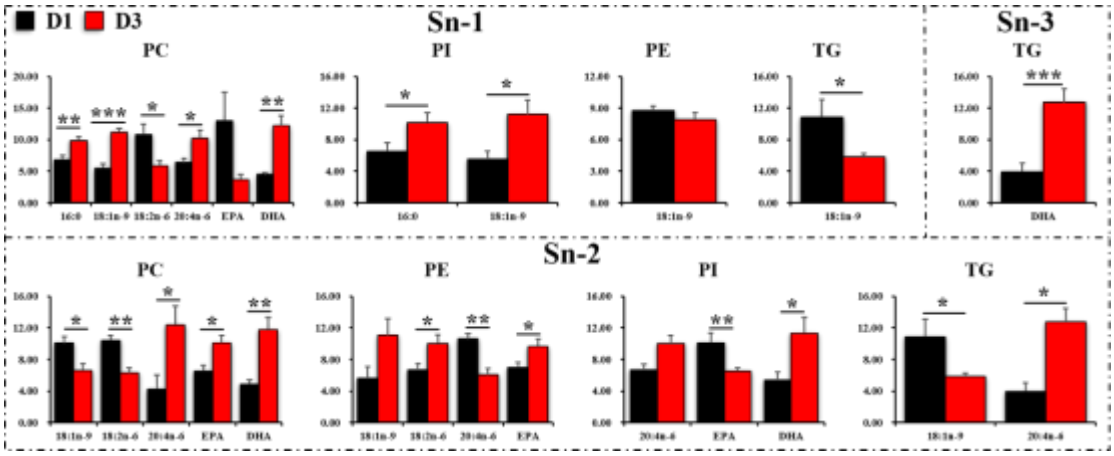

Figure 6. Effects of dietary DHA/EPA ratio on positional distributions of key fatty acids in PC, PE, PI and TG molecules in hepatopancreas of *S.paramamosain* fed with diet D1 and D3. Values are means ± SEM (n = 6). *, ** and *** represent significant differences with $P < 0.05$, $P < 0.01$ and $P < 0.001$.

Supplementary Table1. Formulations and proximate compositions of the experimental diets.

Ingredients	D1	D2	D3	D4
Casein [1]	25.00	25.00	25.00	25.00
Soy protein concentrate [2]	27.61	27.61	27.61	27.61
Wheat flour	25.26	25.26	25.26	25.26
DHA-enriched oil [3]	0.00	1.28	2.57	3.20
EPA-enriched oil [4]	2.96	2.22	1.48	1.11
ARA-enriched oil [5]	0.50	0.50	0.50	0.50
Palmitic acid [6]	1.40	0.86	0.31	0.05
Soybean lecithin	1.00	1.00	1.00	1.00
Cholesterol	0.50	0.50	0.50	0.50
Betaine (98%)	0.10	0.10	0.10	0.10
Vitamin premix [7]	1.00	1.00	1.00	1.00
Mineral premix [7]	1.50	1.50	1.50	1.50
$Ca(H_2PO_4)_2$	2.00	2.00	2.00	2.00
Choline chloride	0.20	0.20	0.20	0.20
Cellulose	8.97	8.97	8.97	8.97
Sodium alginate	2.00	2.00	2.00	2.00
Total	100.00	100.00	100.00	100.00
Proximate composition				
Moisture	7.59	7.81	7.13	6.91
Crude protein	45.69	44.85	45.03	45.08
Crude lipid	7.43	7.85	7.51	7.51
Ash	6.62	6.15	6.26	6.11

[1] Casein: 89.6% crude protein and 0.2% crude lipid.

[2] Soy protein concentrate: 69.9% crude protein and 0.5% crude lipid.

[3] DHA-enriched oil: extracted from marine microalgae, DHA content, 406.5 mg g^{-1} oil (Changsha Kenan Biotechnology Co., Ltd., China).

[4] EPA-enriched oil: extracted from marine microalgae, EPA content, 462.5 mg g^{-1} oil, DHA content, 235.6 mg g^{-1} oil (Changsha Kenan Biotechnology Co., Ltd., China).

[5] ARA-enriched oil: extracted from *Mortierella alpine* (a yeast), ARA content, 468.0 mg g^{-1} oil (Changsha Kenan Biotechnology Co., Ltd., China).

[6] Palmitic acid: Palmitic acid content 97% of total fatty acids, in the form of methyl ester (Shanghai Yiji Chemical Co., Ltd., China).

[7] Vitamin and mineral premixes were based on Jin et al. (2015).

ARA, 20:4n-6; DHA, 22:6n-3; EPA, 20:5n-3.

Supplementary Table 2. Fatty acid contents (mg g^{-1}, dry matter) of the experimental diets.

Fatty acids	D1	D2	D3	D4
14:0	0.56	0.58	0.63	0.65
16:0	10.99	9.70	8.23	7.66
18:0	2.02	2.10	2.12	2.27
20:0	0.20	0.23	0.24	0.26
Total SFA [1]	13.78	12.61	11.22	10.84
16:1n-7	0.20	0.21	0.24	0.25
18:1n-9	5.23	5.84	6.28	6.83
20:1n-9	0.15	0.11	0.11	0.10
22:1n-11	0.05	0.05	0.04	0.04
Total MUFA [2]	5.63	6.21	6.67	7.22
18:2n-6	7.27	7.19	6.90	7.20
18:3n-6	0.23	0.21	0.23	0.24
20:2n-6	0.11	0.08	0.09	0.09
ARA [3]	2.19	2.24	2.12	2.15
22:4n-6	0.16	0.29	0.09	0.07
Total n-6 PUFA [4]	9.97	10.02	9.43	9.75
18:3n-3	1.04	1.02	1.00	1.04
18:4n-3	0.42	0.35	0.24	0.28
20:4n-3	0.42	0.38	0.39	0.42
EPA [5]	10.37	8.18	5.48	4.57
22:5n-3	1.28	1.02	0.68	0.54
DHA [6]	6.45	9.92	12.33	14.49
Total n-3 PUFA [7]	19.98	20.87	20.12	21.35
n-3/n-6 PUFA	2.00	2.08	2.13	2.19
DHA/EPA	0.62	1.21	2.25	3.17
Total n-3 LC-PUFA [8]	18.53	19.50	18.88	20.03

Data are means of duplicate analyses.

[1] SFA, saturated fatty acids: 14:0, 16:0, 18:0, 20:0.

[2] MUFA, monounsaturated fatty acids: 16:1n-7, 18:1n-9, 20:1n-9.

[3] ARA, 20:4n-6

[4] n-6 PUFA, n-6 polyunsaturated fatty acids: 18:2n-6, 18:3n-6, 20:2n-6, 20:4n-6, 22:4n-6.

[5] EPA, 20:5n-3. [6] DHA, 22:6n-3.

[7] n-3 PUFA, n-3 polyunsaturated fatty acids: 18:3n-3, 18:4n-3, 20:4n-3, EPA, 22:5n-3, DHA.

[8] n-3 LC-PUFA, n-3 long-chain polyunsaturated fatty acids: 20:4n-3, EPA, 22:5n-3, DHA.

598 **Supplementary Table 3.** Growth performance of mud crabs fed with the experimental diets.

Diet	Initial Weight (g)	WG (%)	SGR (% d^{-1})	MF
D1	20.62±1.09	44.26±2.83^{c}	0.65±0.04^{b}	0.63±0.19
D2	21.68±1.08	52.85±1.29^{b}	0.75±0.01^{ab}	0.65±0.05
D3	23.38±1.17	62.41±0.49^{a}	0.81±0.01^{a}	1.03±0.10
D4	20.05±1.45	55.80±1.65^{ab}	0.73±0.02^{ab}	0.75±0.11

599 Data are presented as means ± SEM (n = 3). Values in the same column with different superscript

600 letters are significantly different ($P < 0.05$).

601 MF, molting frequency; SGR, specific growth rate; WG, weight gain.

602

Supplementary Table 4. Fatty acid contents (mg g^{-1}, dry matter) of hepatopancreas of mud crabs fed with the experimental diets

Fatty acids	Diet			
	D1	D2	D3	D4
14:0	1.43±0.08^{b}	1.62±0.04^{b}	2.06±0.05^{a}	1.95±0.05^{a}
16:0	21.42±0.11^{b}	26.55±0.76^{a}	25.36±0.45^{a}	23.01±0.48^{b}
18:0	8.53±0.02^{b}	10.11±0.08^{a}	10.22±0.16^{a}	10.00±0.41^{a}
20:0	1.09±0.05^{b}	1.32±0.00^{a}	1.43±0.03^{a}	1.39±0.04^{a}
Total SFA	32.48±0.12^{c}	39.6±0.88^{ab}	39.06±0.69^{ab}	36.35±0.92^{b}
16:1n-7	1.37±0.10^{b}	2.30±0.08^{a}	2.44±0.15^{a}	2.27±0.15^{a}
18:1n-9	19.02±0.19^{b}	21.35±0.54^{b}	25.59±0.56^{a}	24.70±0.85^{a}
20:1n-9	0.59±0.05^{b}	0.90±0.01^{a}	0.78±0.04^{a}	0.80±0.03^{a}
22:1n-11	0.16±0.01^{c}	0.31±0.00^{a}	0.22±0.00^{b}	0.20±0.01^{bc}
Total MUFA	21.15±0.15^{c}	24.86±0.48^{b}	29.02±0.75^{a}	27.97±0.87^{a}
18:2n-6	17.76±0.31^{b}	20.48±0.93^{ab}	21.09±0.44^{a}	19.97±0.76^{ab}
18:3n-6	0.47±0.07	0.65±0.06	0.74±0.01	0.71±0.07
20:2n-6	1.10±0.09^{b}	1.53±0.03^{a}	1.26±0.02^{ab}	1.32±0.06^{ab}
ARA	12.97±0.16^{b}	15.23±0.65^{ab}	15.72±0.10^{a}	14.57±0.95^{ab}
22:4n-6	0.23±0.02^{c}	0.37±0.00^{a}	0.35±0.00^{ab}	0.29±0.03^{bc}
Total n-6 PUFA	32.52±0.47^{bc}	38.26±1.62^{a}	39.16±0.57^{a}	36.86±1.85^{ab}
18:3n-3	1.88±0.13^{b}	2.09±0.13^{ab}	2.41±0.11^{a}	2.20±0.08^{ab}
18:4n-3	0.36±0.05^{b}	0.51±0.03^{a}	0.42±0.01^{ab}	0.33±0.01^{b}
20:4n-3	1.00±0.07^{b}	1.24±0.08^{ab}	1.29±0.03^{a}	1.18±0.05^{ab}
EPA	15.28±0.34^{a}	13.84±0.72^{ab}	14.25±0.33^{ab}	12.18±0.38^{b}
22:5n-3	3.84±0.15^{a}	2.30±0.17^{b}	2.21±0.03^{bc}	1.69±0.07^{c}
DHA	19.04±0.29^{b}	20.96±0.59^{b}	36.08±0.82^{a}	35.36±0.57^{a}
Total n-3 PUFA	42.00±1.03^{b}	40.33±1.74^{b}	56.67±1.26^{a}	52.95±1.09^{a}
DHA/EPA	1.25±0.01^{e}	1.52±0.04^{d}	2.53±0.00^{c}	2.91±0.06^{b}
TFA	128.15±4.01^{c}	143.05±2.17^{b}	163.92±3.27^{a}	154.13±4.65^{ab}

Data are presented as means ± SEM (n = 3). Values in the same row with different superscript letters are significantly different ($P < 0.05$).

ARA, 20:4n-6; DHA, 22:6n-3; EPA, 20:5n-3; MUFA, monounsaturated fatty acid; PUFA, polyunsaturated fatty acid; SFA, saturated fatty acid; TFA, Total fatty acids.

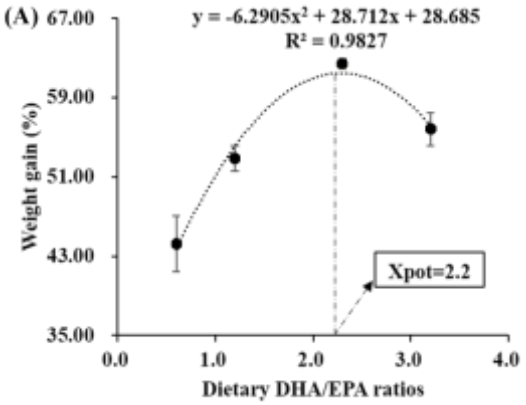

610

611 **Supplementary Figure 1.** Optimum dietary DHA/EPA requirement of mud crab fed with 7% lipid.

612

613

614

615

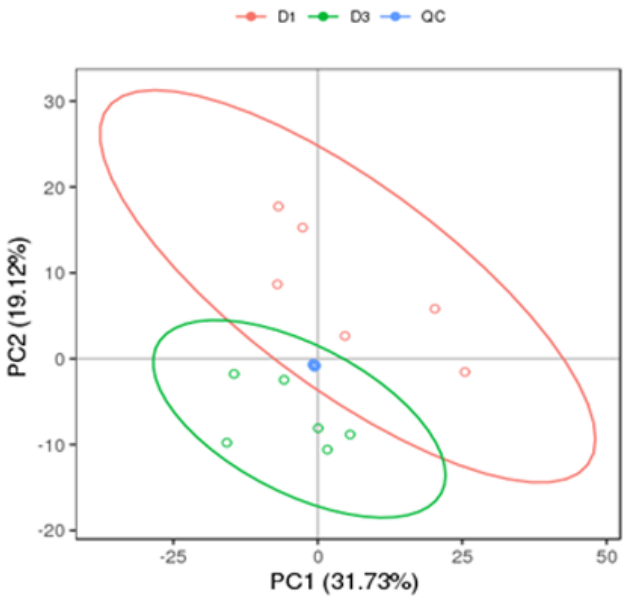

616

617 **Supplementary Figure 2.** Principal component analysis (PCA) plots for quality control (QC)

618 samples. The horizontal axis represents the first principal component, the ordinate axis represents

619 the second principal component, the numbers are the score of the principal component indicating

620 the ability of the principal component to explain the entire model.

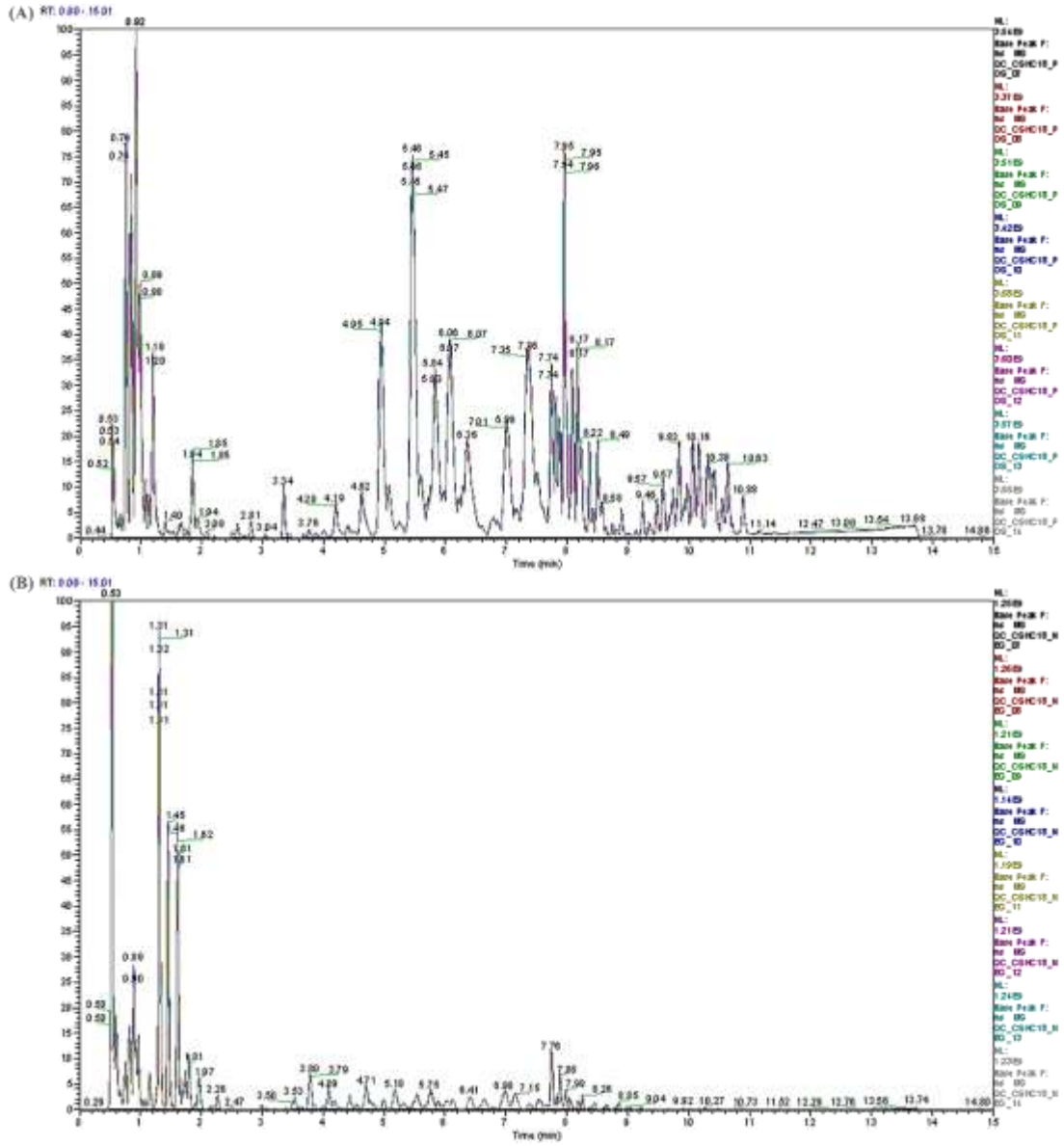

Supplementary Figure 3. The overlap plot of base peak chromatograms (BPC) acquired in positive (A) and negative (B) ionization mode of all the quality control (QC) samples.

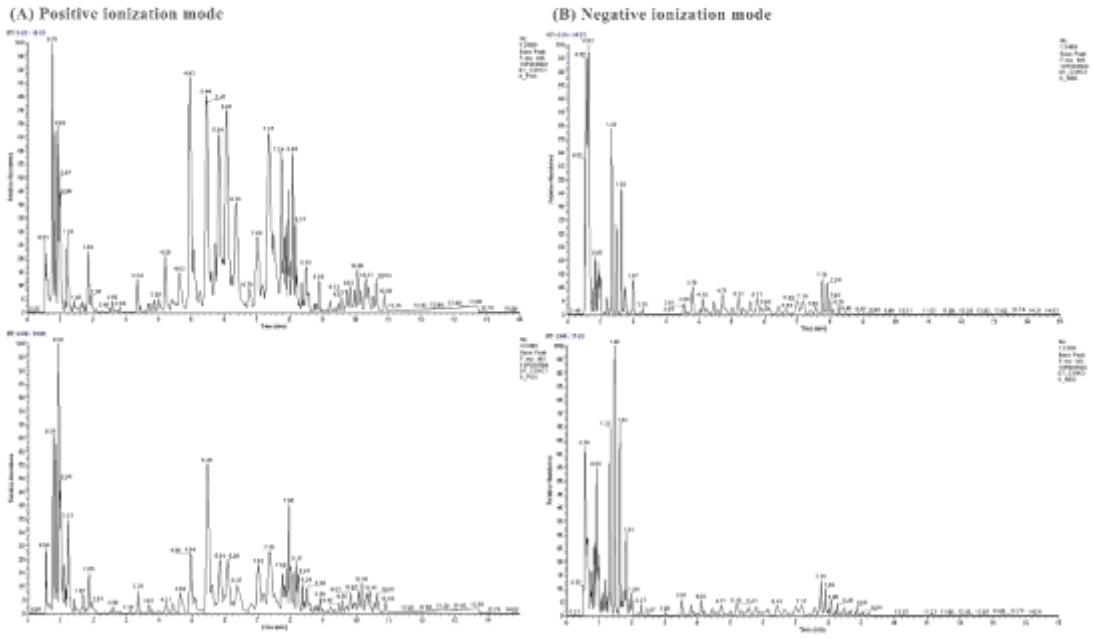

Supplementary Figure 4. The base peak chromatograms (BPC) acquired in positive (A) and negative (B) ionization mode of hepatopancreas of mud crab fed with diet D1 and D3. The spectra of each ionization mode are diets D1 (upper panels) and D3 (lower panels)

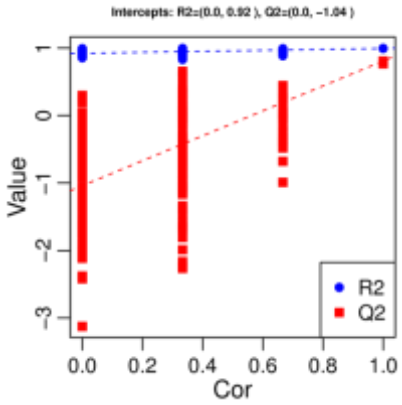

Supplementary Figure 5. Cross-validation plot of the PLS-DA model of all the lipid species. R^2 and Q^2 are the intercepts of the ordinate axis of the regression lines of R^2 and Q^2, Q^2 should be less than 0.

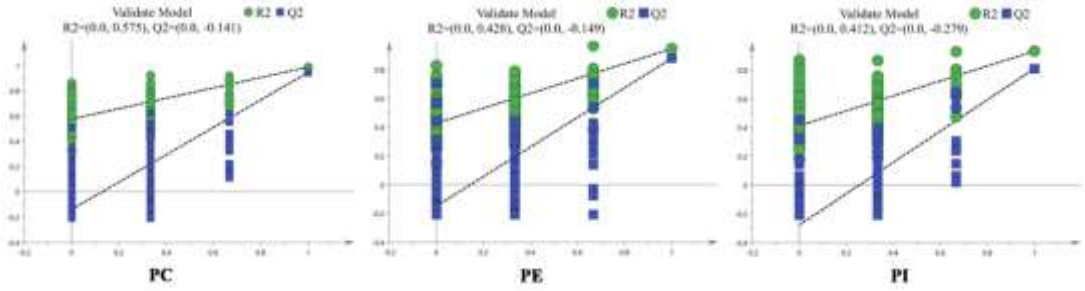

Supplementary Figure 6. Cross-validation plot of the PLS-DA model of PC, PE and PI. R^2 and Q^2 are the intercepts of the ordinate axis of the regression lines of R^2 and Q^2, Q^2 should be less than 0. PC, phosphatidylcholine; PE, phosphatidylethanolamine; PI, phosphatidylinositol.

647